Analytical solutions of the thermal field induced by moving double-ellipsoidal and double-elliptical heat sources in a semi-infinite body

Víctor D. Fachinotti, Andrés Amílcar Anca and Alberto Cardona[*,†]

Centro Internacional de Métodos Computacionales en Ingeniería (CIMEC-INTEC), Universidad Nacional del Litoral (UNL), Consejo Nacional de Investigaciones Científicas y Técnicas (CONICET), Güemes 3450, S3000GLN Santa Fe, Argentina

SUMMARY

An analytical solution is computed for the thermal field induced in a semi-infinite body by a moving heat source whose shape was proposed by Goldak *et al.* for the simulation of welding processes. Owing to its ability to accommodate a wide variety of welding techniques, this model is widely used. Throughout two semi-ellipsoidal volumes, corresponding to the front and the rear parts of the moving source, the heat power density is distributed using a Gaussian function.

In the literature, Nguyen *et al.* have proposed an analytical solution to this problem that is, however, only correct when both semi-ellipsoids are equal (i.e. for a single-ellipsoidal model). The current work presents an extension of the analytical solution of Nguyen *et al.* to the double-ellipsoidal case. As a special case, the solution for the temperature field induced by a double-elliptical surface heat source is also developed.

In order to validate the analytical solutions, the problem is solved using both two- and three-dimensional finite element models in several test-cases. Solutions for double-ellipsoidal and double-elliptical sources are numerically computed and compared with the analytical solutions, while clearly demonstrating the differences with respect to the solution of Nguyen *et al.* At the same time, the two-dimensional numerical approximation is evaluated in terms of accuracy and computational cost. Copyright © 2009 John Wiley & Sons, Ltd.

[*]Correspondence to: Alberto Cardona, CIMEC-INTEC, Güemes 3450, S3000GLN Santa Fe, Argentina.
[†]E-mail: acardona@intec.unl.edu.ar

1. INTRODUCTION

The thermal analysis of a welding process commonly implies the solution of a heat-transfer problem with a highly-concentrated heat source, which is often in motion. In welding numerical analyses, the moving double-ellipsoidal model, proposed by Goldak *et al.* [1], is one of the most widely used heat source models. The model is unique due to its ability to accommodate different fusion welding techniques, which include gas metal arc welding (GMAW) [2–6], gas tungsten arc welding [5, 7–16], shielded metal arc welding [7], submerged arc welding [1], laser spot welding [17], electron beam welding [1, 18], and laser-GMA hybrid welding [19].

Analytical solutions are based on a number of simplifying assumptions (e.g. constant material properties, semi-infinite domain, adiabatic surface, etc.). Therefore, their accuracy is low, especially near the welding pool. Numerical simulation does not need to introduce these simplifying assumptions and for this reason it has been employed more and more.

Although limited to particular situations, analytical solutions are fundamental to the validation of numerical models. In fact, the availability of experimental results is usually required as reference for comparison [1]. However, the double-ellipsoidal heat source model has several parameters for calibration that allow adequately fitting numerical results to experimental data (even for simplified numerical models, e.g. when using a coarse mesh or a large time step). Therefore, in order to assess the accuracy of a finite element model in terms of mesh and time-step size and at the same time find the correct values for the parameters of the Goldak's model, it is more accurate to compare the results of the numerical model with an analytical solution of a representative problem, which will be inherently free of measurement errors.

Nguyen *et al.* [2] developed a closed-form solution of the three-dimensional thermal conduction problem under Goldak's double-ellipsoidal heat source. This solution has been used by several authors to assess the accuracy of a numerical solution and as a basis for the development of other heat source descriptions:

- Nguyen *et al.* [6] developed an analytical solution for the case of welding of a finite-thick plate.
- Recently, for applications to laser material processing, Van Elsen *et al.* [20] proposed a heat source with an analytical solution in a semi-infinite medium.
- Goyal *et al.* [21] proposed a heat source with an analytical solution for pulsed current GMAW.

In all cases, Nguyen's solution was incorporated without correctly accounting for the different sizes of the front and the rear ellipsoids.

In this work, the analytical solution is presented for the problem of heat conduction, induced by Goldak's double-ellipsoidal heat source, in a semi-infinite domain. In contrast to Nguyen's original solution [2], this analytical solution correctly accounts for differences between the front and rear contributions of the double-ellipsoidal heat source.

In addition, the analytical solution is developed for the case of a double-elliptical heat source. This heat source model is well-suited for shallow penetration welds and was previously applied by Lei *et al.* [12] to simulate TIG welding. Other welding models, such as the classical 'disc' model developed by Pavelic *et al.* [22] or the elliptical surface with a Gaussian-distributed heat flux developed by Bang *et al.* [7], can be seen as particular cases of the double-elliptical heat flux model.

Finally, in order to validate the proposed analytical solutions, a welding thermal problem is numerically solved using finite elements. Solutions for double-ellipsoidal and double-elliptical

sources are numerically computed and compared with the analytical solutions, while clearly demonstrating the differences with respect to the solution of Nguyen *et al.* Two-dimensional and three-dimensional numerical models are concurrently used to evaluate the two-dimensional numerical approximation in terms of accuracy and computational cost.

2. MOVING DOUBLE-ELLIPSOIDAL HEAT SOURCE

Consider a fixed Cartesian reference frame (x, y, z), in which a heat source located initially at $z = 0$ and at time $t = 0$, moves with constant velocity, v, along the z-axis. In the case of welding applications, Goldak *et al.* [1] defined the heat source at a position (x, y, z) and time, t, by means of the following double-ellipsoidal distribution:

$$q(x, y, z, t) = \frac{6\sqrt{3}Q}{\pi\sqrt{\pi}ab} \times \begin{cases} \dfrac{f_{\rm f}}{c_{\rm f}} \exp\left[-3\dfrac{x^2}{a^2} - 3\dfrac{y^2}{b^2} - 3\dfrac{(z-vt)^2}{c_{\rm f}^2}\right] & \text{for } z > vt \\[3mm] \dfrac{f_{\rm r}}{c_{\rm r}} \exp\left[-3\dfrac{x^2}{a^2} - 3\dfrac{y^2}{b^2} - 3\dfrac{(z-vt)^2}{c_{\rm r}^2}\right] & \text{for } z < vt \end{cases} \tag{1}$$

where Q is the energy-input rate; a, b, $c_{\rm r}$, and $c_{\rm f}$ are the respective radii of the sides, rear and front of the ellipsoid (see Figure 1); $f_{\rm r}$ and $f_{\rm f}$ are the portion of the heat deposited, respectively, in the front and rear ellipsoid (with $f_{\rm r} + f_{\rm f} = 2$).

Let us note that

$$\int_{-\infty}^{\infty} \int_{-\infty}^{\infty} \int_{-\infty}^{\infty} q(x, y, z, t)\, {\rm d}x\, {\rm d}y\, {\rm d}z = 2Q \tag{2}$$

For arc welding, the energy input rate, Q, can be expressed as

$$Q = \eta V I \tag{3}$$

where η is the arc efficiency, V the voltage and I the current intensity.

In order to fit the results to experimental data, calibration, of the double-ellipsoidal heat source model of Goldak *et al.*, requires adjustment of six parameters: η, a, b, $c_{\rm f}$, $c_{\rm r}$, and $f_{\rm f}$. In the
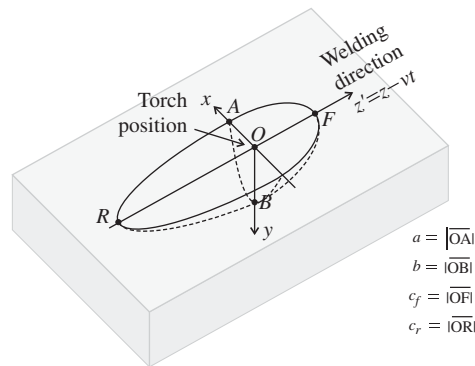
Figure 1. Double-ellipsoidal heat source model.

literature, some authors [2, 6, 13] have reduced the number of free parameters by imposing an additional constraint: $f_f/c_f = f_r/c_r$. This constraint forces continuity of the function q across the $z = vt$ plane at any time, t, to yield

$$f_f = \alpha c_f/(c_r + c_f) \tag{4}$$

with $\alpha = 2$. The literature on modeling of welds has usually ignored this condition; indeed, $\alpha = 2$ was found to lie between 1.8 [1] and 3 [1, 5, 19, 23]. An $\alpha = 3$ correlates with the choice of $c_r = 4c_f$ and $f_f = 0.6$; which, as suggested by Goldak *et al.* [1], should be used as a default value when not enough experimental data are available. Please note that the temperature field induced by the double-ellipsoidal heat source, q, is always continuous (independent of the value of α).

3. TEMPERATURE FIELD

Heat conduction in a homogeneous solid is governed by the linear partial differential equation

$$\rho c \frac{\partial T}{\partial t} - k \nabla^2 T = q \tag{5}$$

where $T = T(x, y, z, t)$ is the temperature at position (x, y, z) and time t, q is the heat source, ρ is the density, c is the heat capacity, and k is the thermal conductivity.

The fundamental solution of Equation (5) is given by the Green function [24]

$$G(x - x', y - y', z - z', t - t') = \frac{1}{\rho c \left[4\kappa\pi(t - t') \right]^{3/2}} \exp\left[-\frac{(x - x')^2 + (y - y')^2 + (z - z')^2}{4\kappa(t - t')} \right] \tag{6}$$

where $\kappa = k/(\rho c)$ is the thermal diffusivity.

Assuming an infinite body with an initial homogeneous temperature, Equation (6) gives the temperature increment at position (x, y, z) and time t due to an instantaneous unit heat source applied at position (x', y', z') and time t'. Then, due to the linearity of Equation (5), the temperature variation induced at position (x, y, z) at time t by an instantaneous heat source of magnitude $q(x', y', z', t')$, which is applied at position (x', y', z') at time t', is

$$q(x', y', z', t') G(x - x', y - y', z - z', t - t') \tag{7}$$

By assuming that the heat has been continuously input at position (x', y', z'), starting from $t' = 0$, the temperature increment at position (x, y, z) at time t is

$$\int_0^t q(x', y', z', t') G(x - x', y - y', z - z', t - t') \, \mathrm{d}t' \tag{8}$$

By adding up all of the heat input contributions, starting from $t' = 0$, that have been made to the entire infinite medium, the temperature increment at any position (x, y, z) and at any time t takes the form

$$\Delta T(x, y, z, t) = \int_0^t \int_{-\infty}^{\infty} \int_{-\infty}^{\infty} \int_{-\infty}^{\infty} q(x', y', z', t') G(x - x', y - y', z - z', t - t') \, \mathrm{d}x' \, \mathrm{d}y' \, \mathrm{d}z' \, \mathrm{d}t' \tag{9}$$

Therefore, the temperature induced by the double-ellipsoidal heat source defined by Equation (1) is

$$\Delta T(x,y,z,t) = \frac{3\sqrt{3}}{4\pi^3} \frac{Q}{\rho c \kappa^{3/2} ab} \int_0^t I_x I_y \left(\frac{f_{\mathrm{r}}}{c_{\mathrm{r}}} I_z^{\mathrm{r}} + \frac{f_{\mathrm{f}}}{c_{\mathrm{f}}} I_z^{\mathrm{f}} \right) (t-t')^{-3/2} \, \mathrm{d}t' \qquad (10)$$

where

$$I_x = \int_{-\infty}^{\infty} \exp\left[-3\frac{x'^2}{a^2} - \frac{(x-x')^2}{4\kappa(t-t')} \right] \mathrm{d}x'$$

$$= 2a\sqrt{\pi} \sqrt{\frac{\kappa(t-t')}{12\kappa(t-t')+a^2}} \exp\left[-3\frac{x^2}{12\kappa(t-t')+a^2} \right] \qquad (11)$$

$$I_y = \int_{-\infty}^{\infty} \exp\left[-3\frac{y'^2}{b^2} - \frac{(y-y')^2}{4\kappa(t-t')} \right] \mathrm{d}y'$$

$$= 2b\sqrt{\pi} \sqrt{\frac{\kappa(t-t')}{12\kappa(t-t')+b^2}} \exp\left[-3\frac{y^2}{12\kappa(t-t')+b^2} \right] \qquad (12)$$

$$I_z^{\mathrm{r}} = \int_{-\infty}^{vt'} \exp\left[-3\frac{(z'-vt')^2}{c_{\mathrm{r}}^2} - \frac{(z-z')^2}{4\kappa(t-t')} \right] \mathrm{d}z'$$

$$= c_{\mathrm{r}}\sqrt{\pi} \sqrt{\frac{\kappa(t-t')}{12\kappa(t-t')+c_{\mathrm{r}}^2}} \exp\left[-3\frac{(z-vt')^2}{12\kappa(t-t')+c_{\mathrm{r}}^2} \right]$$

$$\times \left\{ 1 - \mathrm{erf}\left[\frac{c_{\mathrm{r}}}{2} \frac{z-vt'}{\sqrt{\kappa(t-t')}\sqrt{12\kappa(t-t')+c_{\mathrm{r}}^2}} \right] \right\} \qquad (13)$$

$$I_z^{\mathrm{f}} = \int_{vt'}^{\infty} \exp\left[-3\frac{(z'-vt')^2}{c_{\mathrm{f}}^2} - \frac{(z-z')^2}{4\kappa(t-t')} \right] \mathrm{d}z'$$

$$= c_{\mathrm{f}}\sqrt{\pi} \sqrt{\frac{\kappa(t-t')}{12\kappa(t-t')+c_{\mathrm{f}}^2}} \exp\left[-3\frac{(z-vt')^2}{12\kappa(t-t')+c_{\mathrm{f}}^2} \right]$$

$$\times \left\{ 1 + \mathrm{erf}\left[\frac{c_{\mathrm{f}}}{2} \frac{z-vt'}{\sqrt{\kappa(t-t')}\sqrt{12\kappa(t-t')+c_{\mathrm{f}}^2}} \right] \right\} \qquad (14)$$

Finally, by assuming that the body was initially at the homogeneous temperature, T_0, the temperature field is defined by

$$T(x,y,z,t) = T_0 + \frac{3\sqrt{3}}{\pi\sqrt{\pi}} \frac{Q}{\rho c} \times \int_0^t \frac{\exp\left[-3\frac{x^2}{12\kappa(t-t')+a^2} - 3\frac{y^2}{12\kappa(t-t')+b^2} \right]}{\sqrt{12\kappa(t-t')+a^2}\sqrt{12\kappa(t-t')+b^2}}$$

$$\times [f_r A_{\mathrm{r}}(1-B_{\mathrm{r}}) + f_f A_{\mathrm{f}}(1+B_{\mathrm{f}})] \, \mathrm{d}t' \qquad (15)$$

with

$$A_i = A(z,t,t';c_i) = \frac{\exp\left[-3\dfrac{(z-vt')^2}{12\kappa(t-t')+c_i^2}\right]}{\sqrt{12\kappa(t-t')+c_i^2}} \tag{16}$$

$$B_i = B(z,t,t';c_i) = \mathrm{erf}\left[\frac{c_i}{2}\frac{z-vt'}{\sqrt{\kappa(t-t')}\sqrt{12\kappa(t-t')+c_i^2}}\right] \tag{17}$$

The index, i, denotes front, f, or rear, r.

The time integral in Equation (15) does not have a closed analytical expression; thus, it must be solved by numerical integration. To this end, recursive-adaptive Simpson quadrature was used and the integral was approximated to within an absolute-error tolerance of 10^{-6}.

Remark I
In the solution proposed by Nguyen *et al.* [2], to the same problem, the terms involving B_i are absent. Thus, their solution is only valid when $c_r = c_f$ and $f_r = f_f = 1$.

Remark II
By assuming that the surface $y=0$ is adiabatic and by considering the symmetry of the solution with respect to the plane $y=0$, Equation (15) can also be interpreted as the temperature increment induced by q in the semi-infinite body ($y \geqslant 0$).

4. EXAMPLE OF APPLICATION

With the material and process data listed in Table I, consider the heat conduction problem in a semi-infinite domain ($y \geqslant 0$). Assume that welding starts at position $O(0,0,0)$ and at time $t=0$, and that the welding torch moves with a constant velocity, $v=5\,\mathrm{mm/s}$, along the z-axis.

Three different cases are studied which correspond to different choices of the parameters defining the size and the portion of heat input to the front and rear semi-ellipsoids. In all cases, the fractions of the total heat corresponding to the front and the rear semi-ellipsoids are defined as

$$f_f = 2\frac{c_f}{c_f+c_r} = 2 - f_r \tag{18}$$

This definition forces the heat power density function, q, given by Equation (1), to be continuous at the $z=vt$ plane at any time, t.

In Figure 2, the temperature evolution is displayed for a point located 5 cm from the starting point along the welding axis. The torch is directly over the observed point at $t=10$ s. Figure 3 shows the temperature along the welding axis 10 s after the start of welding (i.e. when the welding torch is located 5 cm away from the starting point).

As the error-function terms in Equation (15) are omitted in the solution proposed by Nguyen *et al.* [2], it is correct only for the cases when $c_f = c_r$ and $f_f = f_r$ (when the error-function terms in Equation (15) cancel themselves). For instance, note that for cases 2 and 3, $c_{f2} = c_{r3}$ and $c_{r2} = c_{f3}$

Table I. Material and process data for a moving double-ellipsoidal heat source in a semi-infinite body.

	Case		
	1	2	3
c_f	15 mm	6 mm	24 mm
c_r	15 mm	24 mm	6 mm
f_f	1	0.4	1.6
ρ		$7820\,\mathrm{kg/m^3}$	
c		$600\,\mathrm{J/(kg°C)}$	
k		$29\,\mathrm{W/(m°C)}$	
T_0		$20°C$	
v		$5\,\mathrm{mm/s}$	
Q		$5083\,\mathrm{W}$	
a		$10\,\mathrm{mm}$	
b		$2\,\mathrm{mm}$	
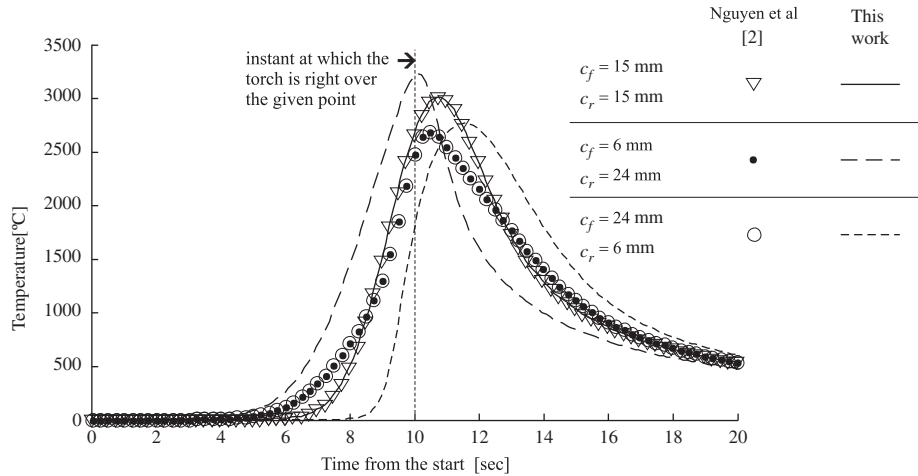
Figure 2. Analytical solutions for the temperature variation with time at position $(0, 0, 5\,\mathrm{cm})$ for the moving double-ellipsoidal heat source.

(i.e. c_f and c_r are interchanged), and also $f_{f2} = f_{r3}$ and $f_{r2} = f_{f3}$ in virtue of Equation (18); then, we get

$$f_{f2}A(z, t, t'; c_{f2}) + f_{r2}A(z, t, t'; c_{r2}) = f_{r3}A(z, t, t'; c_{r3}) + f_{f3}A(z, t, t'; c_{f3})$$

Therefore, the solution of Nguyen *et al.* gets the same answer in both cases, which is clearly not physical.

As it can be observed in Figures 2 and 3, the solutions proposed, in the current study, for the double-ellipsoidal heat source reproduce the expected results when front and rear semi-ellipsoids of different dimensions receive different fractions of the total heat input. As shown in Figure 2, the current solution shows that the temperature increase, induced by the heat source at a given
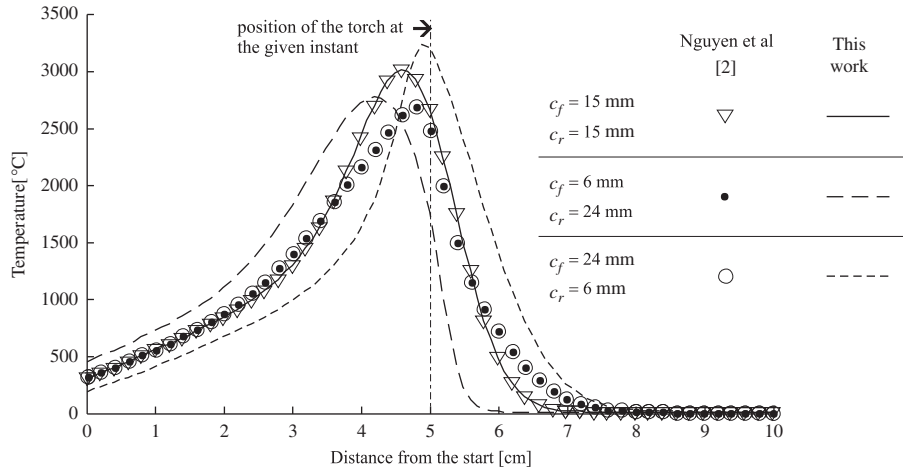
Figure 3. Analytical solutions for the temperature profile along the welding path, 10 s after the start of welding, for the moving double-ellipsoidal heat source.
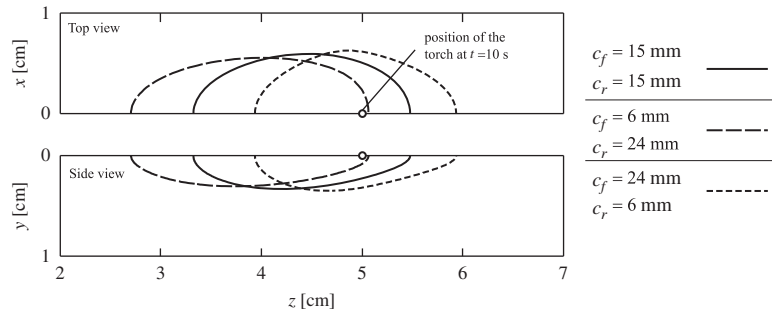
Figure 4. Analytic computation of top and side views of the isotherm of 1560°C, 10 s after the start of welding, for the moving double-ellipsoidal heat source.

point along the welding path, arrives earlier for case 3 than for cases 1 and 2. The earlier arrival of the temperature increase in case 3 is explained by the fact that, in the welding direction, the front semi-ellipsoid of case 3 is longer than those of cases 1 and 2. These solutions are compared in next section with finite element solutions, and an excellent agreement is observed.

Figure 4 displays a top view and a side view of the isotherm of 1560°C, which corresponds to the melting temperature. We can see the effect of changing Goldak's parameters on the position of the welding pool with respect to the torch position.

4.1. Comparison with finite elements solutions

With an analytical solution at hand, the accuracy of two different finite element (FEM) approximations to the problem of heat conduction induced by a moving double-ellipsoidal heat source will be evaluated. In both cases, the fully implicit Euler-backward technique is used for time
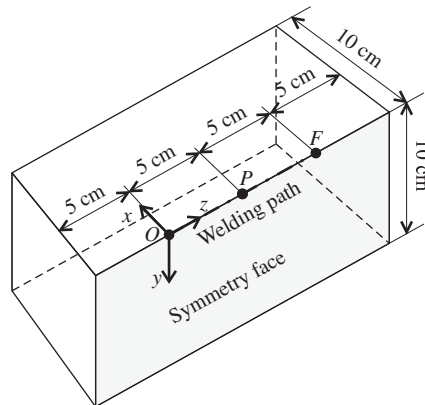
Figure 5. Geometry adopted for the finite element analysis of the temperature induced by a moving double-ellipsoidal heat source in a semi-infinite body.
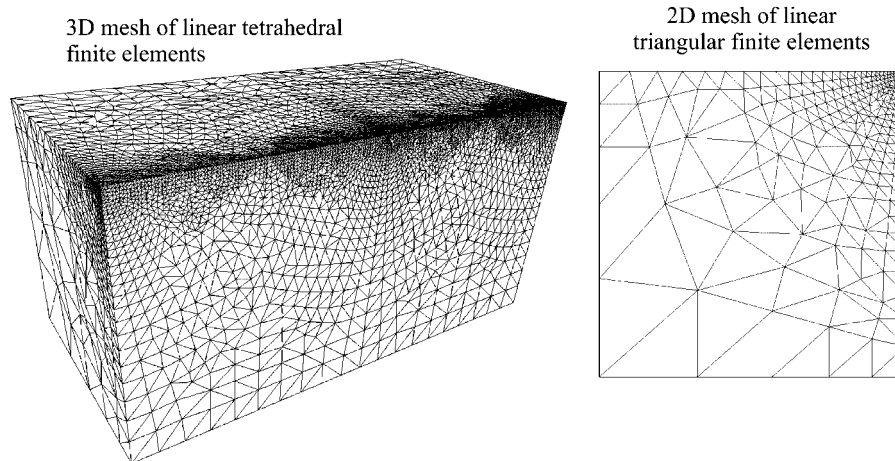
Figure 6. 3D and 2D finite element meshes adopted for the analysis of the temperature induced by a moving double-ellipsoidal heat source in a semi-infinite body.

discretization. Both finite element models are implemented in the OOFELIE code [25], and also include solidification and melting [26, 27].

As shown in Figure 5, the semi-infinite medium is approximated with a hexahedral volume: $0 \leqslant x \leqslant 10$ cm, $0 \leqslant y \leqslant 10$ cm, -5 cm $\leqslant z \leqslant 15$ cm. Welding begins at position $O(0, 0, 0)$ and at time $t = 0$, and follows the path $\overline{OF}$ (symmetry with respect to plane $x = 0$ is assumed).

An unstructured mesh of 65 557 linear tetrahedral elements (13 547 nodes) is used to discretize the domain (see Figure 6 at the left). The mesh is gradually refined towards the welding axis, where the average element size is $h = 0.84$ mm. The time step is set to 0.05 s and kept constant during the analysis.

By assuming a dimensional reduction of the problem to two dimensions, a second finite element solution is computed. In this type of problem, a dimensional reduction is a common method used to reduce the computing time [28, 29]. Usually, two-dimensional models are built by considering either a thin plate, represented by a plane shell where welding is performed, or by making a plane section normal to the welding direction. The latter model is well suited for the case being currently addressed. By assuming that the temperature distribution is stationary (with respect to a coordinate system attached to the torch, which moves at a constant speed, v, along the z-axis), the 3-D temperature field can be determined from the 2-D temperature field using the relationship

$$T(x, y, z, t) = T(x, y, z_{2D}, t + (z_{2D} - z)/v) \tag{19}$$

The accuracy of this model increases with the Peclet number, Pe [30]; which is directly proportional to the welding velocity, v, and to the characteristic dimension in the welding direction, L; and inversely proportional to the diffusivity of the material. Thus, the Peclet number can be represented as

$$Pe = \frac{vL}{\kappa} \tag{20}$$

By adopting $L = 10$ cm, a Peclet number of $Pe = 80.9$ is obtained, which validates the use of the 2-D cross-sectional model.

The cross section located at $z \equiv z_{2D} = 5$ cm is chosen for this analysis. The unstructured mesh of 486 linear-triangular finite elements (280 nodes), as shown at the right of Figure 6, is used. The mesh size is equivalent to that of the 3-D mesh (in fact, the 2-D mesh is the cross section at $z = 5$ cm of the current 3-D mesh). The time step used is 0.05 s.

Next, the results obtained from the numerical models and the analytical solution will be compared. As shown in Figures 7 and 8, for both the temperature evolution at point P and the temperature profile along $\overline{OF}$ at $t = 10$ s (see Figure 5), the 3-D FEM model fits the analytical curves with high accuracy.
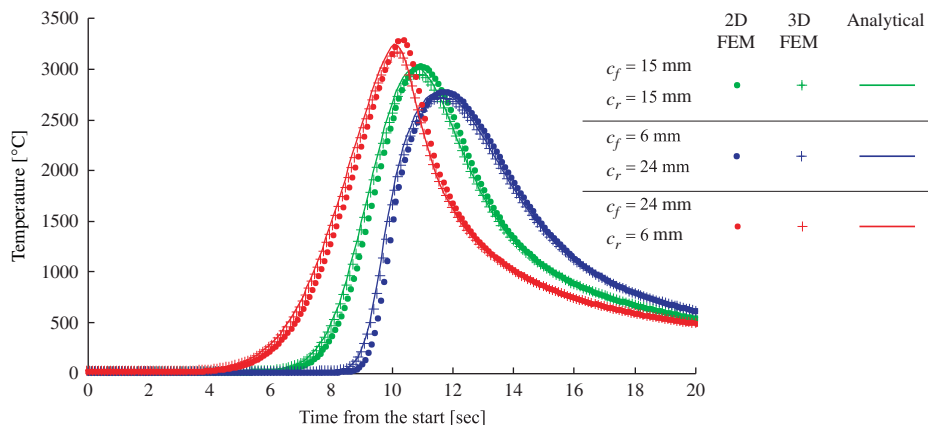
Figure 7. Analytical and FEM solutions for the temperature variation with time, at position $(0, 0, 5\,\text{cm})$, for a moving double-ellipsoidal heat source.
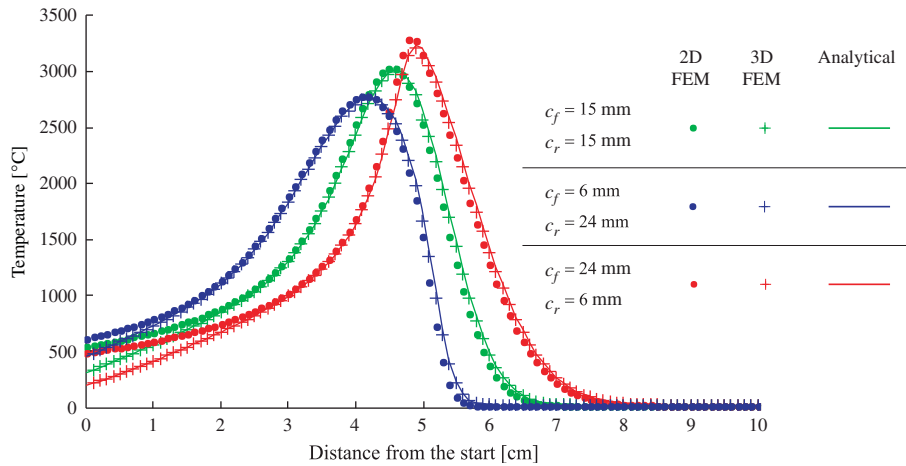
Figure 8. Analytical and FEM solutions for the temperature profile, along the welding path, 10 s after the start of welding, for a moving double-ellipsoidal heat source.

On the other hand, for the entire time interval of interest, the 2-D FEM model gives satisfactory results for the temperature evolution at position P (which is located at the considered cross section). At $t = 10$ s, the temperature predicted along $\overline{OF}$ agrees with the analytical solution, except at the proximity of the starting point of welding. These results coincide with the observation of Goldak *et al.* [28, 29] that the 2-D cross-sectional model is unable to account for run-on effects.

Finally, it should be mentioned that the CPU consumptions of both models are impressively different: 5288 s for the 3-D FEM and 13.7 s for the 2-D FEM (times are reported using a PC with an Intel Core 2 Duo 6300 processor).

5. MOVING DOUBLE-ELLIPTICAL HEAT FLUX

Consider the double-elliptical heat flux model as the limiting case of the double-ellipsoidal one, when the depth of the heat source approaches zero (i.e. $b \to 0$). In this case, the heat power per unit area at the surface $y = 0$ is given by

$$
f(x, z, t) = \lim_{b \to 0} \frac{6\sqrt{3}Q}{\pi\sqrt{\pi}ab} \int_0^\infty \exp\left(-3\frac{y^2}{b^2}\right) dy \times
\begin{cases}
\dfrac{f_{\mathrm{f}}}{c_{\mathrm{f}}} \exp\left[-3\dfrac{x^2}{a^2} - 3\dfrac{(z-vt)^2}{c_{\mathrm{f}}^2}\right] & \text{for } z > vt \\[2ex]
\dfrac{f_{\mathrm{r}}}{c_{\mathrm{r}}} \exp\left[-3\dfrac{x^2}{a^2} - 3\dfrac{(z-vt)^2}{c_{\mathrm{r}}^2}\right] & \text{for } z < vt
\end{cases}
$$

$$
= \frac{3Q}{\pi a} \times
\begin{cases}
\dfrac{f_{\mathrm{f}}}{c_{\mathrm{f}}} \exp\left[-3\dfrac{x^2}{a^2} - 3\dfrac{(z-vt)^2}{c_{\mathrm{f}}^2}\right] & \text{for } z > vt \\[2ex]
\dfrac{f_{\mathrm{r}}}{c_{\mathrm{r}}} \exp\left[-3\dfrac{x^2}{a^2} - 3\dfrac{(z-vt)^2}{c_{\mathrm{r}}^2}\right] & \text{for } z < vt
\end{cases}
\tag{21}
$$

The temperature increment produced by the surface heat flux, defined by Equation (21), is obtained as the limit of the function $T = T(x, y, z, t)$ (given in Equation (15) and evaluated at $y = 0$) when b approaches zero:

$$T(x, z, t) = T_0 + \frac{3\sqrt{3}}{\pi\sqrt{\pi}} Q/(\rho_c) \times \int_0^t \frac{\exp\left[-3\frac{x^2}{12\kappa(t-t')+a^2}\right]}{\sqrt{12\kappa(t-t')+a^2}\sqrt{12\kappa(t-t')}}$$

$$\times \left[f_r A_r (1-B_r) + f_f A_f (1+B_f)\right] dt' \tag{22}$$

with A_f, B_f, A_r, and B_r defined by Equations (16) and (17).

Note: The classical 'disc' model, developed by Pavelic *et al.* [22], can be recovered by setting $f_f = f_r = 1$ and $c_f = c_r = a$, and by defining the concentration coefficient as $C = 3/a^2$. The surface term of the welding heat input, used by Bang *et al.* [7] (where heat flux is defined using a Gaussian function over an elliptical surface) can be obtained by taking $f_f + f_r = 1$ and $c_f = c_r$.

5.1. Example of application

Consider the problem of determining the temperature induced by a welding source, modeled as a double-elliptical heat flux, moving with constant speed, v, along the z-axis. The geometry, material, and welding parameters are the same as those of Section 4, except for the depth of the ellipsoids, b, which is zero.

Fully 3-D and 2-D cross-sectional finite element analyses are performed using the same space and time discretization as in the double-ellipsoidal heat source case.

Numerical and analytical results are shown in Figures 9 and 10. Concerning the accuracy of 3-D and 2-D cross-sectional finite element approximations, current results confirm those found in Section 4.1. The 3-D FEM model fits the analytical curves with high accuracy, while the 2-D cross-sectional model is accurate to predict the temperature evolution at points located over the analyzed section but the accuracy deteriorates for points located far from this section.

We remark that in the double-elliptical surface model, the heat power is more concentrated than in the double-ellipsoidal volume heat model. Thus, for a given total heat input, Q, the temperatures induced by the former are considerably higher than those induced by the latter.

6. CONCLUSIONS

In this work, an analytical solution was proposed for the problem of unsteady thermal conduction in a semi-infinite medium (induced either by a double-ellipsoidal moving heat source or a double-elliptical heat flux). This problem is of great industrial interest since it is representative of a wide variety of welding processes on thick plates.

For the first time, an exact analytical solution is given for the case of double-ellipsoidal (or double-elliptical) heat sources, with different values of size or heat input for the front and rear subregions. The proposed solution corrects a previous solution proposed in the literature, which was used by several authors as a basis in the following applications: finite-thick plate welding analysis [6], pulsed current GMAW [21], and laser material processing [20]. The solution that this current work presents can be easily extended to these applications by following the work made by these authors.
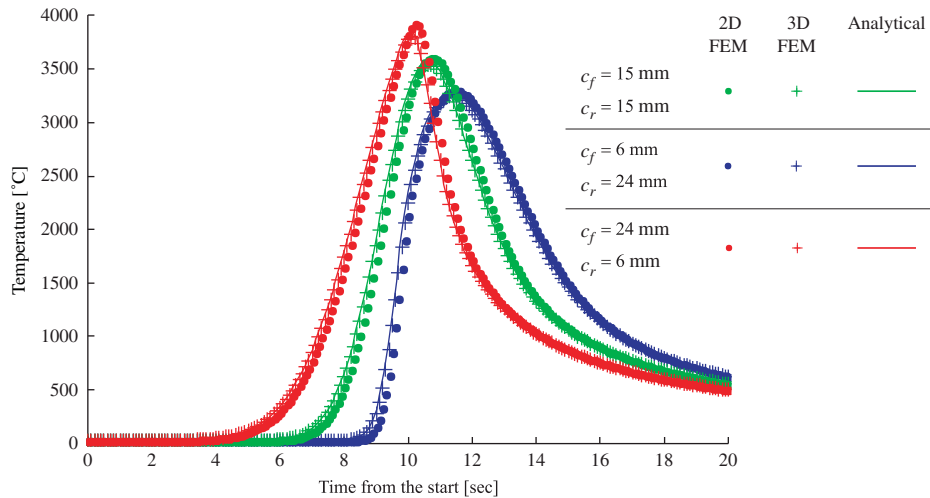
Figure 9. Analytical and FEM solutions for the temperature variation with time, at the position $(0, 0, 5\,\text{cm})$, for a moving double-elliptical heat flux.
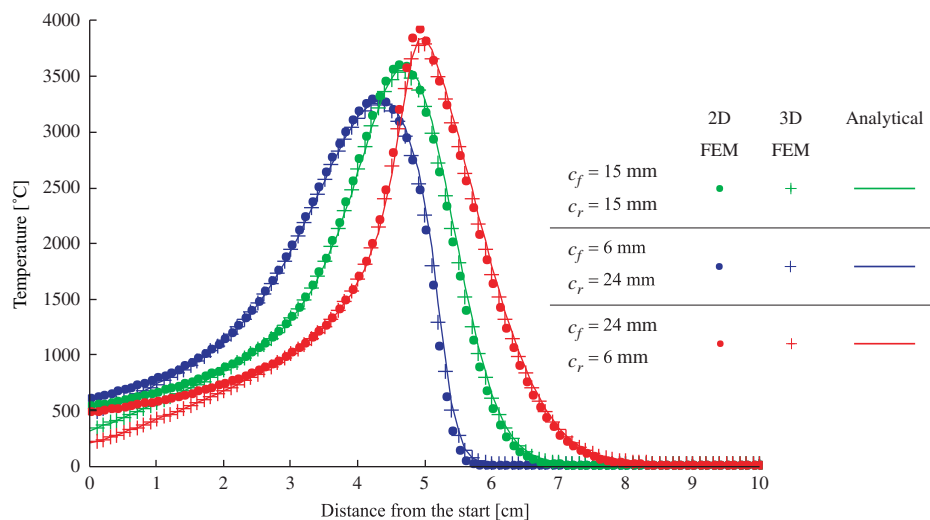
Figure 10. Analytical and FEM solutions for the temperature profile along the welding path, 10 s after the start of welding, for a moving double-elliptical heat flux.

The availability of an analytical solution permits the evaluation of a numerical solution free of experimental uncertainties. As validation examples, the finite element numerical solutions in both the 3-D and the simplified 2-D cases were computed and compared with the exact analytical solutions. The examples also demonstrated that 2-D computations give very accurate solutions (when the analysis position is located far from the welding zone extremes) with a minimum consumption of CPU time.

REFERENCES

1. Goldak J, Chakravarti A, Bibby M. A new finite element model for welding heat sources. *Metallurgical Transactions B* 1984; **15**:299–305.
2. Nguyen NT, Ohta A, Matsuoka K, Suzuki N, Maeda Y. Analytical solutions for transient temperature of semi-infinite body subjected to 3-D moving heat sources. *Welding Research Supplement* 1999; **78**:265–274.
3. Abid M, Siddique M. Numerical simulation to study the effect of tack welds and root gap on welding deformations and residual stresses of a pipe-flange joint. *International Journal of Pressure Vessels and Piping* 2005; **82**:860–871.
4. Abid M, Siddique M, Mufti RA. Prediction of welding distortions and residual stresses in a pipe-flange joint using the finite element technique. *Modelling and Simulation in Materials Science and Engineering* 2005; **13**:455–470.
5. Gery D, Long H, Maropoulos P. Effects of welding speed, energy input and heat source distribution on temperature variations in butt joint welding. *Journal of Materials Processing Technology* 2005; **167**:393–401.
6. Nguyen NT, Mai Y, Simpson S, Ohta A. Analytical approximate solution for double ellipsoidal heat source in finite thick plate. *Welding Journal* 2004; **83**:82–93.
7. Bang I-W, Son Y-P, Oh KH, Kim Y-P, Kim W-S. Numerical simulation of sleeve repair welding of in-service gas pipelines. *Welding Journal* 2002; **81**:273–282.
8. Branza T, Duchosal A, Fras G, Deschaux-Beaume F, Lours P. Experimental and numerical investigation of the weld repair of superplastic forming dies. *Journal of Materials Processing Technology* 2004; **155–156**:1673–1680.
9. Deng D, Murakawa H. Prediction of welding residual stress in multi-pass butt-welded modified 9Cr1Mo steel pipe considering phase transformation effects. *Computational Materials Science* 2006; **37**:209–219.
10. Deng D, Murakawa H. Numerical simulation of temperature field and residual stress in multi-pass welds in stainless steel pipe and comparison with experimental measurements. *Computational Materials Science* 2006; **37**:269–277.
11. Duranton P, Devaux J, Robin V, Gilles P, Bergheau JM. 3D modelling of multipass welding of a 316L stainless steel pipe. *Journal of Materials Processing Technology* 2004; **153–154**:457–463.
12. Lei Y-C, Yu W-X, Li C-H, Cheng X-N. Simulation on temperature field of TIG welding of copper without preheating. *Transactions of Nonferrous Metals Society of China* 2006; **16**:838–842.
13. Lundbäck A, Alberg H, Henrikson P. Simulation and validation of TIG-welding and post weld heat treatment of an inconel 718 plate. In *Proceedings of the 7th International Seminar on the Numerical Analysis of Weldability*, *Graz-Seggau*, Austria, Cerjak H, Bhadeshia HKDH, Kozeschnik E (eds), 2003.
14. Thiessen RG, Richardson IM, Sietsma J. Physically based modelling of phase transformations during welding of low-carbon steel. *Materials Science and Engineering A* 2006; **427**:223–231.
15. Wu CS, Yan F. Numerical simulation of transient development and diminution of weld pool in gas tungsten arc welding. *Modelling and Simulation in Materials Science and Engineering* 2004; **12**:13–20.
16. Wu CS, Chen J, Zhang YM. Numerical analysis of both front- and back-side deformation of fully-penetrated GTAW weld pool surfaces. *Computational Materials Science* 2007; **39**(3):635–642.
17. De A, Maiti SK, Walsh CA, Badheshia HKDH. Finite element simulation of laser spot welding. *Science and Technology of Welding and Joining* 2003; **8**(5):377–384.
18. Goldschmied G, Tschegg EK, Schuler A. Electron beam surface melting-numerical calculation of the melt geometry and comparison with experimental results. *Journal of Physics D*: *Applied Physics* 1990; **23**:1686–1694.
19. Reutzel EW, Nelly SM, Martukanitz RP, Bugarewicz MM, Michaleris P. Laser-GMA hybrid welding: process monitoring and thermal modeling. *Proceedings of the 7th International Conference on Trends in Welding Research*, *2005*, Pine Mountain, U.S.A., 2005.
20. Van Elsen M, Baelmans M, Mercelis P, Kruth JP. Solutions for modelling moving heat sources in a semi-infinite medium and applications to laser material processing. *International Journal of Heat and Mass Transfer* 2007; **50**:4872–4882.
21. Goyal VK, Ghosh PK, Saini JS. Analytical studies on thermal behaviour and geometry of weld pool in pulsed current gas metal arc welding. *Journal of Materials Processing Technology* 2009; **209**(3):1318–1336.

22. Pavelic V, Tanbakuchi R, Uyehara OA, Myers PS. Experimental and computed temperature histories in gas tungsten arc welding of thin plates. *Welding Journal Research Supplement* 1969; **48**:295S–305S.
23. Song J, Peters J, Noor A, Michaleris P. Sensitivity analysis of the thermomechanical response of welded joints. *International Journal of Solids and Structures* 2003; **40**:4167–4180.
24. Carslaw HS, Jaeger JC. *Conduction of Heat in Solids* (2nd edn). Oxford University Press: Oxford, 1959.
25. Open Engineering. OOFELIE::Multiphysics, 2008.
26. Fachinotti VD, Cardona A, Huespe AE. A fast convergent and accurate temperature model for phase-change heat conduction. *International Journal for Numerical Methods in Engineering* 1999; **44**:1863–1884.
27. Fachinotti VD, Cardona A, Huespe AE. Numerical simulation of conduction–advection problems with phase change. *Latin American Applied Research* 2001; **31**:31–36.
28. Goldak J, Bibby M, Moore J, House R, Patel B. Computer modelling of heat flow in welds. *Metallurgical Transactions B* 1986; **17**:587–600.
29. Goldak JA, Akhlaghi M. *Computational Welding Mechanics*. Springer Science+Business Media, Inc.: New York, 2005.
30. Mendez PF. Joining metals using semi-solid slurries. *Master's Thesis*, Department of Materials Science and Engineering, Massachusetts Institute of Technology, 1995.